

EXPERIMENTS ON THE PLASTIC DEFORMATION OF THIN METAL PLATES UNDER BLAST TYPE LOADING

by
Kenkichi KIYOTA*

I. INTRODUCTION

1. The diaphragm gauge.

Plastic deformations of thin metal plates under shock pressure of explosion have been used as a diaphragm gauge for the purpose of measuring the effective strength of explosives.

In order to measure the effectiveness of the explosion impact we had to resort to many indirect methods, one of which is to use a diaphragm gauge applied often as a blastmeter. Formerly its final deformation was supposed to give a measure of the peak pressure of the explosion.

According to Cole's "Underwater Explosion"¹⁾, such a gauge was first developed by an Italian Mondugo about 1919. Another type of diaphragm gauge is the British "pot" gauge and a modified form was used for the comparisons of explosives in America. Bebb²⁾ published in 1945, an improved type shown in Fig. 1. In most cases, the diaphragm was ordinarily made of steel or copper and is clamp-

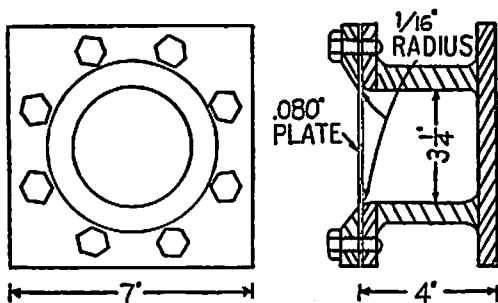


Fig. 1 UERL diaphragm gauge

received Dec. 10, 1967

* Kumamoto University

ed to the gauge body by a face plate. In practice the gauge is placed at a known distance from the explosive and the nearly hemispherical deformation resulting from the impact is taken as a measure of explosive effectiveness largely for empirical comparisons.

In Germany another type of blastmeter — "Bleimembranmessdose" — was developed by the Chemisch-Technisch Reichsanstalt³⁾, and many papers about it were published there by W. Gliwitzki⁴⁾, W. Hoffmann und G. Meier⁵⁾ and H. Busch⁶⁾. Fig. 2 shows the blast meter devised by H. Busch in 1959. They used mainly a lead plate, and rarely an aluminum or copper plate, as the diaphragm.

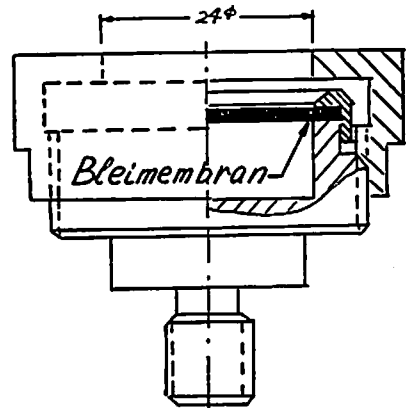


Fig. 2 Bleimembran-Meßdose

The late Dr. Yamaga⁵⁾ introduced the blast meter in this country which is shown in Fig. 3a and its performances were studied by Suzuki⁹⁾ and Fukuyama.¹⁰⁾

The diaphragm gauges developed in Italy, England and U.S.A. are mostly of the clo-

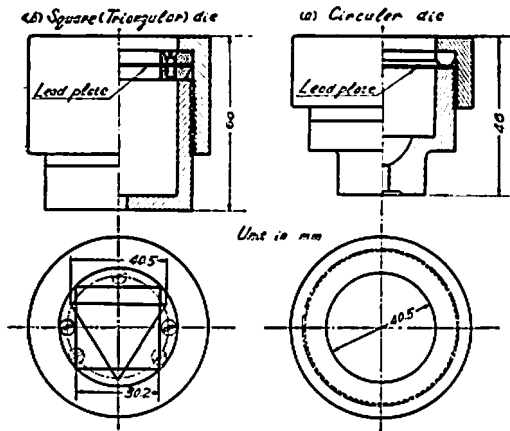


Fig. 3 The diaphragm gauge

sed chamber type and mainly for underwater experiments. Those developed in Germany and Japan are characterized by the use of the open chamber and are intended to be used mainly in the air.

2. The peculiar shape of the permanent deformation of the plate.

R. H. Cole and others analysed the permanent deformation of the thin metal plate under the explosive pressure, especially of underwater explosion, on the assumption that the deformed plate had always a semi-spherical profile, and this was proved to be true by their experiments. In many experiments on fluid cupping test or hydraulic bulge test¹¹⁾, the thin metal plate fixed on the circular rigid boundary deforms permanently into semi-spherical form when it is subjected to a hydrostatic pressure above a certain limit. This seems also to have been supported by the analysis of the plastic deformations.¹¹⁾

However, there are some other types of deformation of plates under explosive impact. The author owes the information to Prof. H. Sudo who told him about an experiment in open air in which the plate of the blastmeter was deformed into conical, not semi-spherical shape under a detonation pressure of a comparatively small charge. This caused the author's concern as it contradicted the

usual notion we had at that time of the plastic deformation of thin metal plates under uniform pressure. So the author repeated the same experiments in open air and then undertook also a new kind of experiment to throw some light on the mechanism of plastic deformations of thin metal plates under the blast load. While it is an established fact that the diaphragm is deformed into a semi-sphere by a certain underwater explosion, it is undeniable that the same is not always the case in open air experiments. There must therefore be some difference of mechanism between them which we need to clarify. It appeared to be necessary to prove that when a thin metal plate is deformed plastically into a cone, the dynamical features of deformation could be probably different from that of the static hydraulic bulge test. Our new experiments also needed to show that the detonation pressure never concentrate at the center of the plate in spite of the conical shape produced by it. In fact, the pressure is always distributed over the plate as will be seen from the following description of our experiments.

As already pointed out by R. H. Cole, even in the case of the permanent semi-spherical deformation, its maximum height is not a simple function of the maximum pressure of shock wave by explosion. What mechanical quantity should be related to the maximum height of the deformed cone of the thin metal plate? What is its main difference from the case of semi-sphere? These questions will be clarified in the following description of the experiments and their mathematical analysis.

II. EXPERIMENTS

3. Experiment I, preliminary test.²²⁾

The blastmeter as shown in Fig 3a which has been used commonly in Japan in the comparison of the explosive effectiveness, is set on the ground. A cylinder of casted TNT

of 30 mm. in diameter, containing 50 grams, is held in the air by a fine wire in such a way that the direction of the axis of cylinder coincides with the axis of the blastmeter. The distance between the plate and the explosive, which is chosen to give moderate permanent deformation on the former, is between 10 cm. and 30 cm. As the material of the diaphragm, copper, brass or mild steel is also applicable. However, lead is the most often used in Japan. Some permanently deformed figures of those plates after explosive blasting are shown in Photo. 1, all of which are conical and quite different from the ones by the fluid-cupping tests. From these photographs it may be concluded that such a peculiar permanent deformation is not to be attributed to the special property of lead, but that it is common to all ductile metals.

It must be considered also that shock wave pressure distribution around the cylindrical charge is not uniform. It rather concentrates on its axis near the charge, and then the shock wave front decays gradually into a sphere with the lapse of time. Therefore, several blastmeters which were set on the ground, and pointed to several other directions than the axis of explosive cylinder, were tested simultaneously by a single blasting explosion. Even in such arrangements, all lead plates of the gauges deformed conically, though the maximum depression on the gauge occurred at the axis of the charge. This test shows that shock wave pressure by explosion of the cylindrical charge does not concentrate so severely as to give a concentrated load at the center of the diaphragm, but, at least qualitatively, it affects the diaphragms in all directions in quite a similar manner.

Next the diaphragm gauges of special type were tested. They had the diaphragms fixed on the peripheries of a square or a regular

triangle, instead of a circle. Under such arrangements, the flat plates deformed into a square pyramid or a regular triangular pyramid instead of a cone, as shown in Photo. 1.

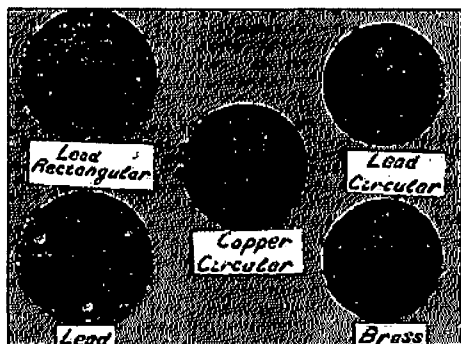


Photo. 1 Deformations of the diaphragms into sand heap form

4. Experiment II, by explosive blasting.²⁵⁾

After acquiring this preliminary knowledge, effects of bending on plastic deformation, magnitude of shear deformation, and the condition of the surface in regard to its crystalline structure after deformation under explosive or static pressure were examined on the deformed lead plate of the gauge.

4. 1. The construction of the diaphragm gauge:

The type of diaphragm gauge as shown in Fig. 3a, was employed as the standard, which is generally used in Japanese industry and is always to be used here unless otherwise noticed. The face plate of the gauge shown in Fig. 3b was reconstructed so as to fix the square or the regular triangular plate instead of the standard circular plate. Each of these was mad of mild steel.

4. 2. Arrangements of explosives and the gauges:

Four arrangements of the explosives and the gauges used in this experiment are shown in Fig. 4 and Fig. 5. In all these cases the axis of the gauges and cylindrical charges were set to coincide with each other, but a special position of the explosive in relation

to the gauge spared the weight of explosive and reduced danger in the experiment. The distance between the surface of the plate and the tip of explosive is called explosive distance and denoted by d . Let us call the four arrangements as follows:

a) An open air method, shown in Fig. 4a, is adopted usually in this country to compare explosive effectiveness.

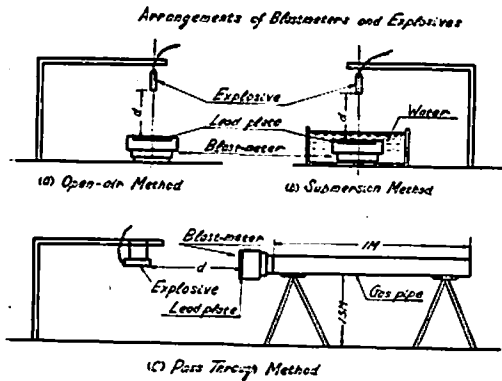


Fig. 4 Arrangement of blastmeters and explosives

b) In the submersion method, shown in Fig. 4b, the gauge is submerged with 5 cm. water head upon the plate in the steel basin; which has the depth of 9 cm. and the inner diameter of 22 cm. Such an arrangement aims first at preventing the small particles, which have been generated in the decomposition of explosive, from colliding with the plate, and next at equalizing the shock wave distribution over the plate.

c) In the pass-through method, shown in Fig. 4c, a gauge which has no bottom and has a male screw on the outside of the bottom, is screwed into the gas pipe, which has the length of 2 m. and is held horizontally at the height of about 1.5 m. from the ground. Such an apparatus has the advantage that even if the plate does not cover a hole in the face plate and a part of the shock wave that has arrived at the gauge passes through freely, it is not reflected from the bottom,

and consequently the deformed figure of the plate by the first shock wave is not further affected by the reflected shock wave.

d) In the duct method, shown in Fig. 5, the gauge is put on the sands in contact with one end of the steel pipe 585 cm. long and 5 mm. thick, setting their axis in line. Into the other end of the pipe, a tin plate pipe of 35 mm. diameter and of 0.5 m. ~ 2.5 m. length, is inserted partly, and in the other end of the tin plate pipe is set an explosive. All of these are covered with sand. In this arrangement explosion always destroys the tin plate pipe, and every time a new pipe must be supplied. In this case the shock wave propagates mainly in one direction through the pipe and decays so slowly that the thickness of the shock front may grow up to more than tenfold of that by a simple spherical shock wave, and therefore the duration of the shock wave pressure on the diaphragm is more than tenfold of that in the open air method. In this method, the explosive distance was chosen to be between the range of 6 m. to 8 m. so as to gain the same height of deformation of the plate as in the open air method.

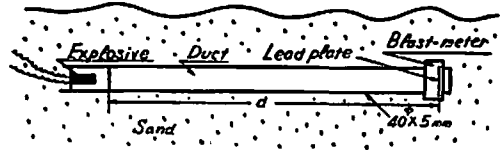


Fig. 5 Arrangement in duct method

e) A static pressure method was also tried to compare the figures of deformation of the diaphragms, as shown in Fig. 6. To the plate of the gauge, oil pressure was applied by the hand oil pump and kept constant for 20 minutes, and then released; thereafter the permanent set of deformation of the plate was measured, because lead creeps largely even at room temperature.

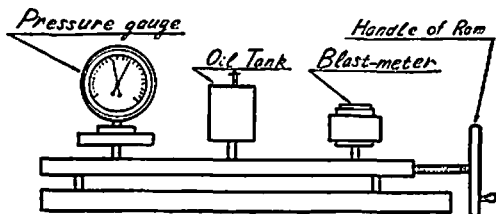


Fig. 6 Arrangement in static pressure method

f) In the repeated blast method, explosive pressure was applied to one specimen repeatedly by the open air method, and after each explosion the measurement of the deformation and heat treatments of lead plate were repeated, with the purpose of observing the process of deformation.

4. 3. Properties of lead plate:

In this experiment the diaphragm was made of lead, which was adopted as an representative of ductile metals, for it deforms easily by weak shock wave. Its specification is as follows:

- a) Purity: 98.63%
- b) Procedure of manufacturing the specimen plate:

A lead plate of about 3 mm. thickness was rolled alternatively in two normal directions by the hand roll into the thickness of about 1.5 mm. and 0.6 mm.

- c) Annealing: heated to $100^{\circ} \pm 5^{\circ}\text{C}$. for about 3 hours and then cooled slowly.
- d) Tensile strength: about 160 kg/cm^2 .
- e) Elongation: about 47%

4. 4. Explosives employed:

a) Unless otherwise noticed, trinitrotoluene (TNT) was always used to simplify the comparison of the results. Its large strength of explosion permits selection of a large explosive distance to produce a sufficient depression of the plate. Thus the diaphragm would be expected to receive a more uniform shock wave pressure, and to minimize the chances to be impaired by the small particles

generated at explosion. TNT powder was put into the cylindrical paper sheath of 32 mm. diameter and of 100 mm. length, retaining a constant density of 0.95.

Several other explosives, which have a large detonating velocity, were also used to compare their effectiveness with that of TNT.

As detonator, an electric detonator was employed.

4. 5. Measuring apparatus:

Direct measurements of shock wave pressure and its duration were tried by using the piezo-electric method and by using a wire resistance strain gauge attached to the metal bar. However, satisfactory results scarcely having been obtained, no description will be made about these in this paper. In our experiment, the following measuring methods were employed.

To measure the permanent deformation of the plate, four concentric circles, the diameter of which were respectively 10 mm., 20 mm., 30., and 40 mm., and cross lines intersecting each other at the center at right angle were drawn on the back surface of the plate before the test. After the deformation the diameters and the heights at their cross points were measured using slide calipers.

The change of the thickness of the plate was measured by the special dial gauge, which was attached to the large arm of horse-shoe from and had a pointed nose to contact the deformed surface of the double curvature at a point.

The micro-structures of the surfaces of the permanently deformed plate either dynamically by blasting or statically by tension test, were transferred on the celluloid plates by the Sump method and inspected by the microscope.

4. 6. Results measured:

a) The deformed section of a lead circular plate of 1.5 mm. initial thickness, after being blasted by an explosive pressure of 50 gram

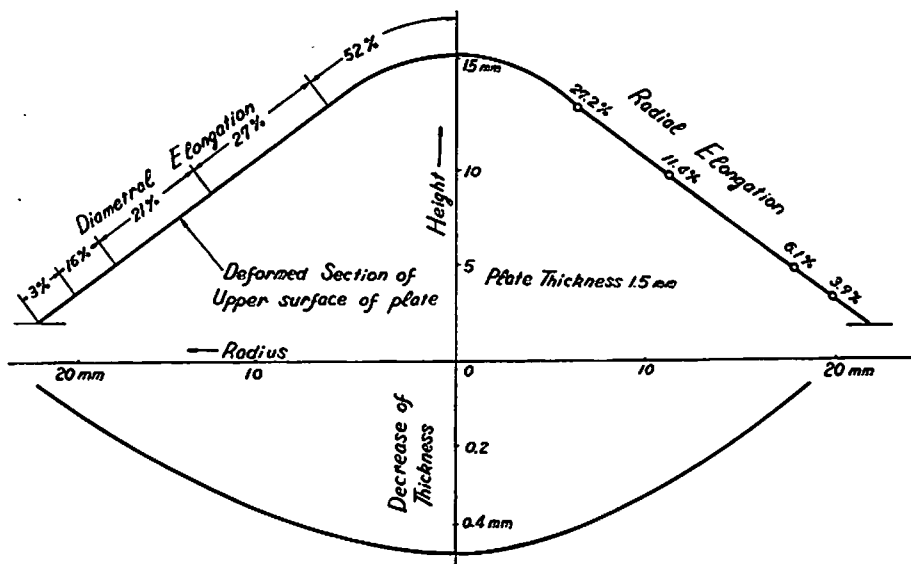


Fig. 7 Deformed section of lead circular plate by open air method

TNT at the explosive distance of 40 cm. by the open air method, is shown in Fig. 7, in which the diametral and circumferential elongations of the concentric circles and also the decrease of the plate thickness along the radius are shown. The diametral and circumferential elongation and the decrease of the thickness increase gradually toward the center and reach maximum at the center.

b) The sections of the six deformed plates by the submersion method, each of which has undergone the explosion pressures of the three sorts of explosives severally, are shown in Fig. 8. all of these sections which are nearly conical, have a little parabolic deviation. This difference is supposed to be due to the fact that the shock wave pressure on the plate by the submersion method is lower at its peak, and longer in duration than those by the open air method.

c) Lead bars of rectangular cross section of 5 mm. width and of 1.5 mm. or 0.6 mm. thickness were tested by the pass-through method. The side views of the plastically deformed bars are shown in Fig. 9, each of which is nearly an equilateral triangle. The

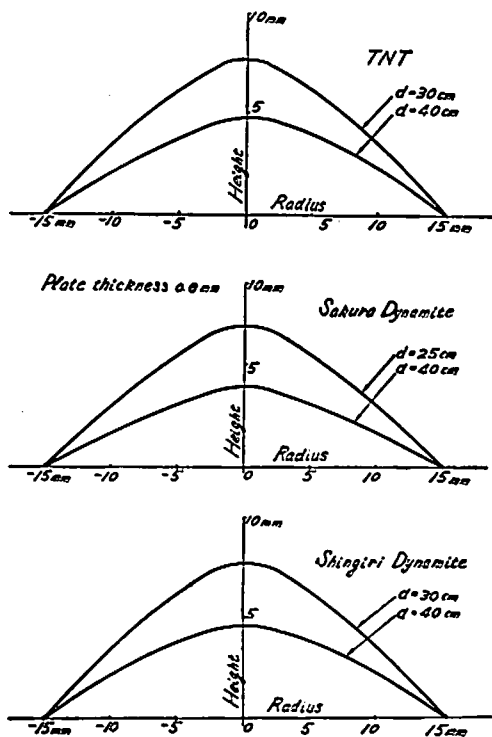


Fig. 8 Deformed section of lead circular plate by submersion method

distributions of axial elongation and decrease in width are generally uniform, while the decrease of the plate thickness clearly increases toward the middle point and reaches maximum at the center. The assemblage of the deformed

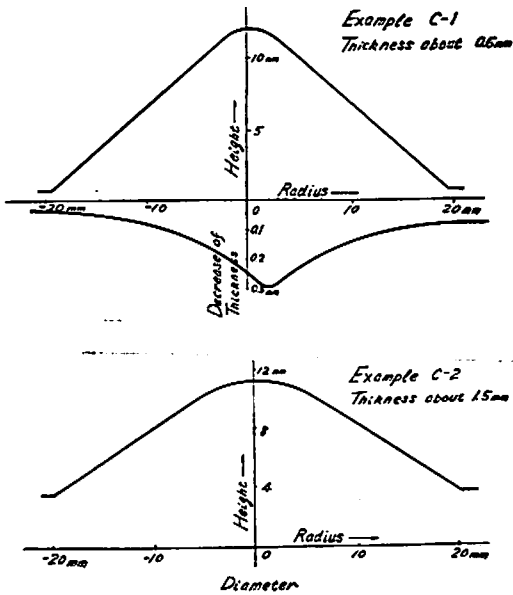


Fig. 9 Deformed section of rectangular bar of lead by pass through method



Photo. 2 Deformed bar by the pass-through method

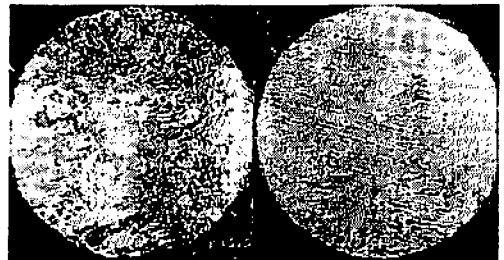
bar and the gauge body in the pass-through method is shown in Photo. 2.

Before the test parallel lines, in a direction perpendicular to the axis of the bar, were carved at equal space of 2mm. on the side of the specimen, which was then set on the blast-meter and tested by the pass-through method. Thereafter, the parallelism of those lines was examined on the deformed specimen, and was perceived to remain the same in the straight part of the specimen. This shows that the shearing deformation is very small compared with the plastic axial elongation as shown in Photo. 3.



Photo. 3 Deformation in shear of the rectangular bar

d) The micro-structures of the surfaces of the two plastically elongated specimens, one of which was tested by the open air method and the other of which was pulled beyond the yield point to about 30 % elongation by the static tension test, were examined by the Sump method. Their micro-photographs are shown in Photo. 4, each of which shows cracks similar to each other on their surfaces. Although the cracks on the static tensile specimen are mostly perpendicular to the direction, of tension those on the specimen tested by the open air method are reticulated, and indicate that the specimen have been pulled in all directions.



(a) Tested by the open air method (b) Pulled by the static tension

Photo. 4 Cracks on the surface of the deformed plate examined by the Sump method

e) To ascertain that the shock wave pressure on the diaphragm gauge has the nonconcentric distribution, five circular lead plates of 1.5 mm. thickness with a concentric hole were used as diaphragms in the pass-through method. The concentric holes on the five specimens had a diameter of 5.4 mm., 7.4 mm., 10.2 mm., 13.0 mm. and 18.7 mm. respectively before the test. The deformed figures of these specimens after the test at the 20 cm. explosive distance are shown in Photo.

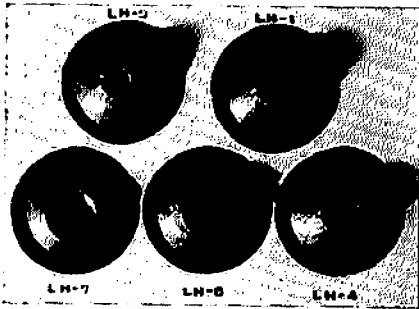


Photo. 5 Deformed figures of lead circular plates with a center hole by the pass through method



Photo. 6 Deformed profile of the circular lead plate with a center hole by the pass through method

5. and Photo. 6, which show us that these specimens have deformed, similarly to the circular plate without a hole, into a frustum of a cone. It is to be noticed here that all the inclinations of generation lines of the cones were almost constantly 40° in spite of the different diameters of the holes. When the circumferential elongation of the plate with a hole is compared with that of the plate without a hole, we know that the former is larger than the latter near the hole, but their difference decreases along the radius and reaches the minimum at the fixed periphery of the plate. This experiment also excludes the supposition that the shock wave pressure of explosion imposed upon the diaphragm concentrates at its center.

f) Next the diaphragm was made rectangular (45 mm. \times 25 mm.) and oval-shaped (two semi-circles of 15 mm. radius connected with a rectangle of 20 mm. \times 30 mm.) in the open-air method. An rectangular plate of 0.5

mm. thickness was tested at the explosive distance of 48 cm. and deformed into a roof shape, showing clearly a ridge, as shown in Photo. 7. An oval-shaped plate of 0.5 mm. thickness was blasted at the explosive distance of 48.5 cm. and its figure after the test was like that of a sand heap on the oval plate, as shown in Photo. 8b.



Photo. 7 Roof shape deformation of the rectangular plate

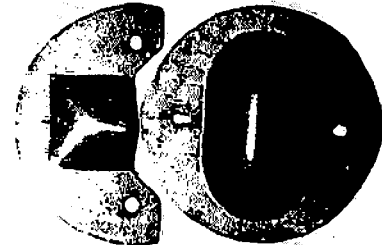


Photo. 8 Deformed figures of the rectangular plate (a) and the oval plate (b)

g) In the next experiment a rectangular diaphragm, the effective area of which was 22.5 mm. \times 25 mm., was held tightly by the face plate of the gauge, the rectangular hole of which was 25 mm. \times 45 mm. Accordingly one side of 25 mm. length of the plate was free and the other three sides were fixed to the gauge. This was blasted by the pass-through method. The deformed figure is shown in Photo. 8a, and it is seen that this has the same form as a half of that shown in Photo.

7. Though the four slopes of the figure of Photo. 7 are nearly equal, in the figure of Photo. 8a the slope opposite to the free side is clearly larger than those generated in the other two fixed sides. The reason probably lies in the fact that the free side of the diaphragm moves easily to the opposite side as the deformation progresses.

h) As an example of a deformed diaphragm tested by the duct method, Fig. 10 is shown. Now, the plate is 1.5mm. in thickness and the explosive distance is 6 m. The figure is semi-spherical and quite resembles that in Fig. 11, which shows the deformed figure of the plate tested by the static method.

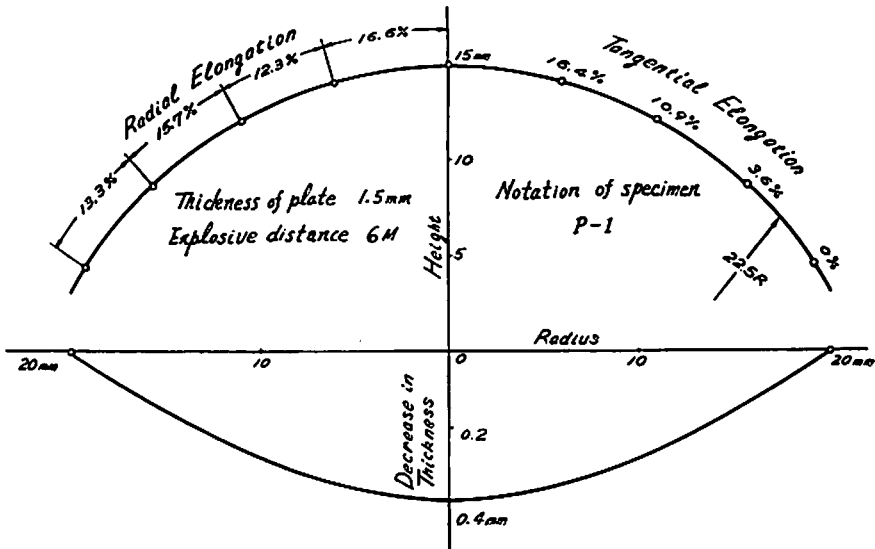


Fig. 10 Deformed section of lead circular plate by the duct method

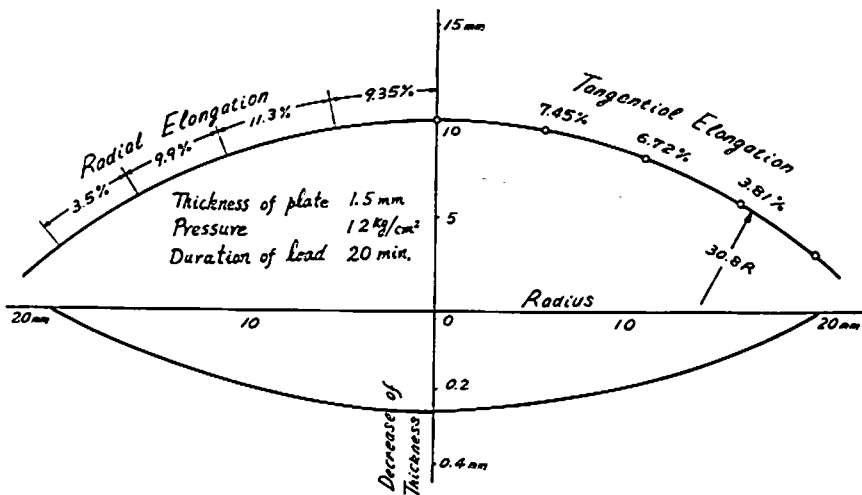


Fig. 11 Deformed section of lead circular plate by the static pressure method

The circular lead plates with different concentric holes were tested by the duct method, one of which is shown in Photo. 9,

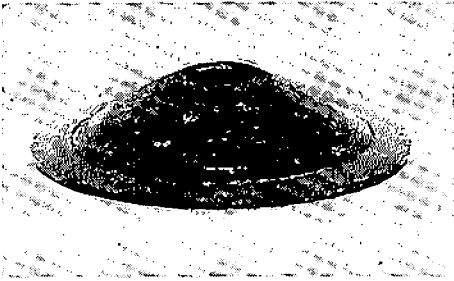


Photo. 9 Deformed figure of the lead circular plate with a center hole by the duct method

and every one showed a semi-spherical shape similar to that of the plate without a hole.

To examine the effect of spherical expansion of shock wave in the duct method, the end of the steel pipe was kept apart from the diaphragm at the distance of 5 cm. or 10 cm. The deformed cross sections of these diaphragms are shown by the curves of A-1 and A-2 in Fig. 12, where the cross-section of Fig. 10 is added as P-1 to compare them with the zero distance section. In accordance with the increase of the distance between the diaphragm and the end of the pipe, the deformed shape goes from semi-sphere to cone.

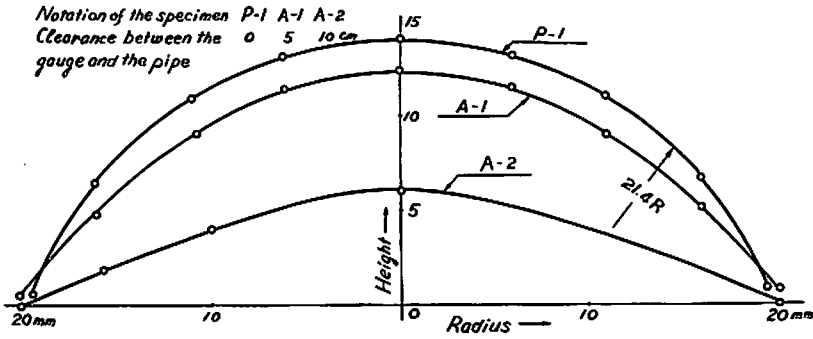


Fig. 12 Effect of clearance between the gauge and the pipe on the deformation

i) Fig. 13 shows the results by the repeated blast method, in which the explosive distance was held always at 35 cm. and explosions were repeated seven times and the seven curves in that figure show the seven

deformed shapes measured after the respective explosions. This figure shows that the conical shape gained at the first explosion swells little by little at every explosion lastly to expand into the semi-sphere.

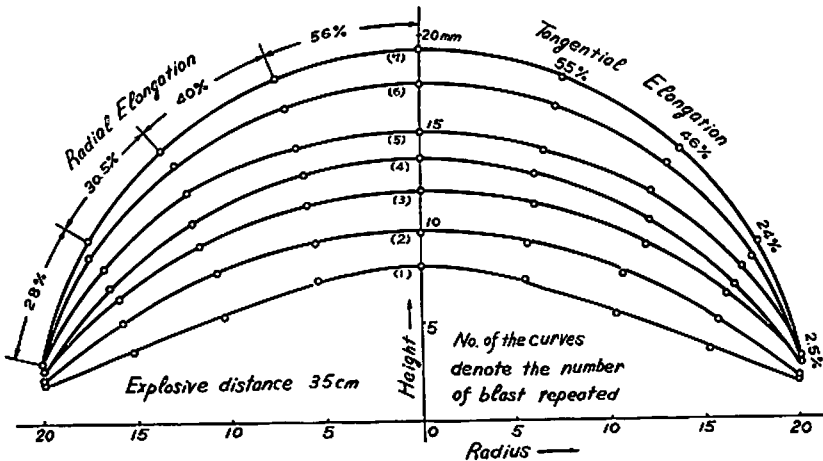


Fig. 13 Change of deformed sections of the lead circular plate by the repetition of explosion

4.7. Experimental results:

From the above experiments, the following conclusions have been deduced:

a) The peculiar shape of the deformation of the diaphragm, when it is blasted by the strong shock wave pressure of explosion, is similar to the sand heap form on the plate, and is common to plastic deformation of ductile metal plates. But we showed not to attribute it to a special property of lead.

b) The supposition that the concentration of shock wave pressure at the center of the diaphragm may cause the deformation of sand heap form on the plate is excluded.

c) Plastic shearing deformation was not perceived, except in the case in which, at the fixed boundary, a large plastic shearing deformation occurs by too strong explosion pressures, as shown in Photo. 6.

d) The measurement of the elongation distribution of the plate and the observation of the microscopic structure of the deformed surface show that the plate is severely elongated in all directions leaving no trace of compression, and the micro-structure of the deformed plate is similar to that gained by the static tension test. Thus, under such a loading condition, the diaphragm may be treated as a membrane, in which bending resistance and shearing deformation can be neglected.

e) The results of the duct method and the repeated blast method show that even the shock wave pressure, when it continues longer than the total period of deformation, gives the diaphragm the deformation of semi-sphere shape similar to that gained by the static test, and an intermediate duration gives an intermediate form.

f) Summing up, we are led to a supposition about the process of deformation of the diaphragm of the gauge to be as follows:

On generating the deformation of sand

heap type, the shock wave pressure of explosion acts during a short interval of time compared with the time required for the total deformation of the plate, and collides with it uniformly to give a uniform normal velocity to the plate. The plate given with the uniform normal velocity collides against the rigid periphery fixed to the gauge body. Thus, the plastic deformation starts at the fixed periphery and then proceeds to the center of the plate, the central part, which has not been reached by the deforming wave, remaining flat.

5. Experiment III, by high-speed camera.^{24) 25)}

From the above experiments we have reached a conclusion about the process of deformation of the thin metal plate of the blastmeter, as was already described. Concerning the problem of the mechanism of the diaphragm into the peculiar shape, it was expected that important facts would be obtained by taking a photograph of the deforming process of the plate by a high speed camera. Therefore, the author planned with the cooperation of Prof. H. Sudo and Prof. T. Uemura to take photographs of the deformations of the diaphragm gauge using high speed camera, which had been invented twenty years before by Prof. T. Suhara¹²⁾ and had the highest speed obtainable in Japan then.

It was just at that time that we came in possession of G. E. Hudson's paper¹³⁾ in which the same problem had been treated. Encouraged on one hand by the agreement of opinion and discouraged on the other hand by his, not my, having taken an initiative in regard to mathematical analysis, as well as by his precedence in revealing the secret physical feature which had so far been hidden of the cone-frustum formation, we set forth in search of the experimental evidences which had been lacking in Hudson's paper. It would

not be inappropriate to mention here that our ideas were developed when we were working at the University of Tokyo, independently of the American investigation.

5.1. Photographing preparations:

By our preliminary test it was found that the time necessary for the total deformation of the lead diaphragm was about 0.5 ms.~1 ms. Therefore in order to take about 10 photographs on the processes of the plate deformation, the high speed camera to be used must have the speed of about 20,000 frames a sec. There being no better one, we decided upon Suhara's camera, which had been installed in the Laboratory of the Research Institute of Science and Engineering. The machine had the highest speed of 40,000 frames a sec. and was available for our use by the cooperation of Prof. T. Uemura and his colleagues.

a) Arc-light was focused by the lens on the concave mirror, and its reflecting beam the silhouette of the deforming figure of the diaphragm was projected on the camera. The camera was too heavy to be moved, so that it was fixed in the building. To avoid the danger of explosion pressure, the apparatus for deforming the plate was set up outside the building. Therefore, the focal distance of 9 m 60 cm. being necessary, a telescopic lens of Tessar 1:5, $F:70$ cm. was used. This arrangement is shown in Fig. 14.

b) To take the photographs of the silhouette of the deforming plate by the open air

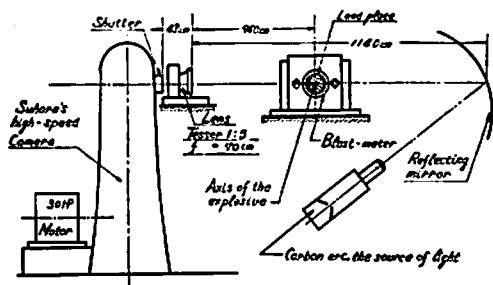


Fig. 14 Arrangement of high-speed photographing

method, the face plate of the gauge was reconstructed so as to let the upper surface of the plate coincide with that of the face plate. This apparatus is shown in Fig. 15. Also, in order to test a rectangular bar by the pass-through method, a new blastmeter was constructed, which had a span of 46 mm. and is shown in Fig. 16.

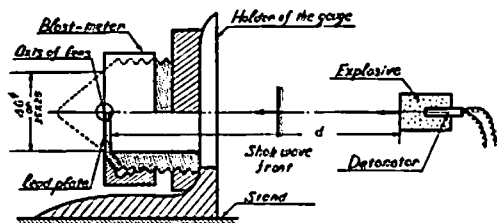


Fig. 15 The special blast-meter to take a silhouette photograph of the deforming plate

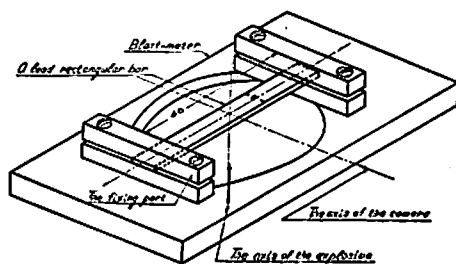


Fig. 16 The new blastmeter to test a rectangular bar

c) The specimens tested were made of ordinary pure lead on the market, and rolled to the thickness of about 0.5 or 0.6mm. Heat treatments of the specimens were omitted, because their effects on the deformed shape were not recognized. On the profile of the specimen the small projections of solder were soldered at intervals of 5 mm., to catch the local deformation of the plate at different stages on the photographs.

d) To prevent injuring the surroundings by explosive pressure, the minimum charge of TNT was determined at 10 gram by the preliminary tests which had been made to give accurately the necessary deformed height to the plate. TNT powder was pressed in a die into a 25 mm. cylinder of 15 mm. length.

by pressure of 1 ton/cm². In the pass-through method, the sphere of 15 mm. diameter made of Shingiri dynamite of 15 gram was used to prevent the explosion from yielding too much smoke, which might cover the figure of the deforming at the moment of photographing, because Shingiri dynamite generated least

smoke.

5.2. Photographs taken:

Four photographs of the deforming diaphragm taken by this apparatus are given here as the representatives. The conditions of photographing and the sizes of the specimens used in these tests are shown in Table I

Table 1 The condition of high speed photographing

Photo. No.	Photo. 10	Photo. 11	Photo. 12	Photo. 13
Plate thickness	0.49mm	0.59mm	0.61mm	0.59mm
Shape of the plate	circular plate 46mm ϕ	circular plate with a hole 46mm ϕ	rectangular plate 35 \times 25mm	Bar fixed at the both ends 6 \times 46mm
Number of Frames/s	22,500	22,700	22,500	22,500
Explosive used	TNT 10gr	TNT 10gr	TNT 10gr	Shingiri dynamite 15gr
Explosive distance	40cm	39cm	42cm	20cm
Detonator used	No. 6 Electric without bottom	do	do	do

a) Photo. 10 shows the deforming process of the lead circular plate of 0.49 mm. thickness by the explosion pressure of 10 gram of TNT. And it made clear that the plastic deformation of the diaphragm started at the fixed boundary and proceeded to the center of the plate, leaving the central part flat and ending on the arrival of deformation at the center, thus yielding a triangle profile, as was expected. The interval of the small projections near the boundary of the plate was observed in the photograph while the conical part was being formed. As the result the increase of its intervals was perceived to be more than 20%.

b) Photo. 11 is the deforming profile of the lead circular plate with a center hole of 10 mm. diameter, and in this case too, the process of deformation was similar to that of the circular plate without a hole. However, as was supposed in this test, the radial velocity of the deforming plate was larger than that of the plate without a hole, and

this photograph shows that in process of deformation the inner periphery of the hole was torn up and bent to the outside by its inertia force. Its deformed shape is shown in Photo. 14.

c) Photo. 12 shows the varying silhouettes of the deforming rectangular plate, viewed from the direction of the shorter side of the plate; these silhouettes are similar to those in the former two, but in the finally deformed figure the ridge of the hipped roof, has a little roundness instead of straight line, probably owing to the periphery of the diaphragm having slid out of the fixed boundary in consequence of loose fitting. The small projections of solder on the plate were most clearly photographed in this among the four. It is noticed that the interval of the projections on the central flat part varies too little to be measured in the photograph.

d) Photo. 13 shows the similar process of deformation of the rectangular bar, but the undeformed central flat part does not



Photo. 10 Process of deformation of the circular plate



Photo. 11 Process of deformation of the circular plate with a center hole



Photo. 12 Process of deformation of the rectangular plate

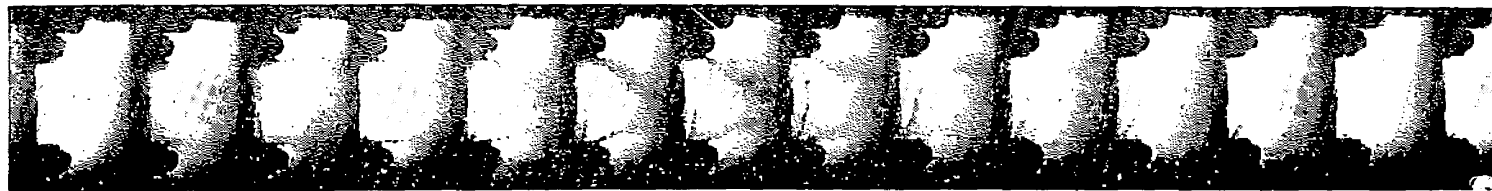


Photo. 13 Process of deformation of the rectangular bar



Photo. 14 The deformed shape of the lead circular plate with a centerhole

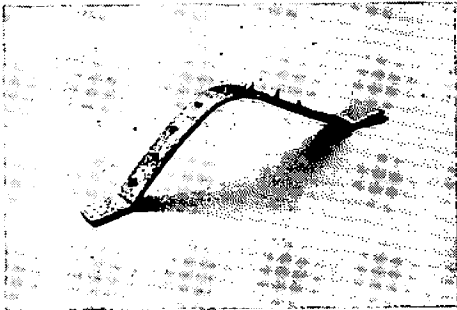


Photo. 15 The deformed shape of the lead rectangular bar

appear so clearly as in the former three cases. This fact will be explained by the fact that the energy of plastic deformation in this bar propagates in one direction and does not concentrate at the center as in the former three, and by the fact that the bar has been slackened initially because, in fixing the bar to the gauge, it was elongated by pressing both ends of the bar, and therefore no sharp

plastic deformation occurred at the fixed ends. The final shape of the deformation bar is shown in Photo. 15, which is a triangle, with a slightly rounded top.

5.3. Analysis of the experimental results:

In the enlarged photographs of Photo. 10, Photo. 11 and Photo. 12, the deformations of a circular plate, and the same with and without a center hole, and of a rectangular plate were measured, comparing them with the dimension of the fixed part which was known as a constant. Duration of deformation was between 0.4 ms. and 0.7 ms. The displacements of the central flat parts from their original positions in these three photographs, and the decrease of the radius of the undeformed central flat part in Photo. 10 were measured. From these data the velocity of translation of the blasted plate and the rate of the radius decrease of the central flat part could be calculated. These results are given in Table 2 and Fig. 17. The figure shows that the diaphragm was first accelerated during a period of about 0.1~0.2 ms. to reach a constant velocity with which it advanced for 0.3~0.4 ms., and then stopped. The radius of the central flat part did not decrease with a constant rate, but decreased in proportion with the 1.25 power of time.

However the velocity was nearly constant between No. 2 frame and No. 6 frame of

Table 2 The results of high-speed photographing

Unit. mm	Photo No.	Frame No. Shape of plate	Frame No.											Time of total deformation in ms
			1	2	3	4	5	6	7	8	9	10	11	
Height of the central flat part	10	Circular plate	0.7	1.4	2.3	3.4	4.9	6.0	7.1	8.4	9.8	10.9	11.4	0.58
	11	Circular plate with a hole	0.2	0.6	1.8	3.0	4.4	5.6	6.9	8.6	10.2	12.8	\	0.40
	12	Rectangular plate	0.6	1.9	3.5	5.2	6.6	8.4	—	—	12.8	\	\	0.36
Decrease of radius of central flat part	10	Circular plate	0.9	2.1	3.4	4.7	6.2	7.7	9.4	12.0	14.6	\	\	\

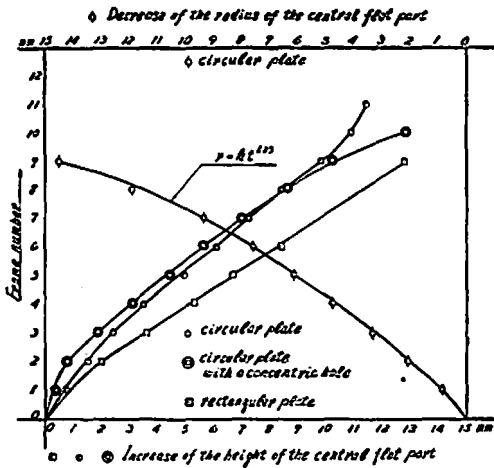


Fig. 17 Variation of the height and radius of the central flat part

Photo. 10, and was about 31.4 m/s, which may be regarded as the velocity of plastic deformation wave along the radius of the plate.

The intervals of the projections on the plate were measured in these photographs, but the change of the distances in the deforming process seems to have been too irregular to give any qualitative conclusion, except that interval of the projections on the uttermost part of the cone had been increasing during the growth of the cone, so that an increase of 20% of their distance at the end of total deformation has resulted.

If the equation of $C_b = (\sigma_Y / \rho)^{1/2}$ holds between the yield point σ_Y and the velocity of plastic deformation wave C_b , where ρ is density of the material used, the dynamic yield point σ_{YD} may be calculated, using the velocity of 31.4 m/s, as follows:

$$\sigma_{YD} = C_b^2 \times \rho = 1.14 \text{ kg/mm}^2$$

By the static tensile test the yield point of lead σ_Y was 0.67 kg/mm², and σ_{YD} was larger by 70% than σ_Y , as is to be expected from the known results of the high-speed tensile tests⁽⁴⁾.

6. Experiment IV, by mechanical impact.^{26) 28)}

The author has ascertained by his experiments described above that the plastic deformation of the blastmeter proceeds exactly as he expected with the mechanism theoretically anticipated. From these he has immediately been led to the conclusion that such peculiar deformation of the diaphragm should be generated not only by the blasting pressure of the explosive, but also by the sudden change of the blastmeter, which, for example, is able to be induced by the collision of the falling gauge with a rigid body, as Hudson's paper has suggested. Although the direct measurement of the magnitude of shock wave pressure generated by the explosion of explosives, or its duration, is very hard at present, to measure the mechanical impact caused by the collision of two rigid bodies is relatively easier. If the deformation of the diaphragm of the gauge by mechanical impact is similar to the sand heap form on the plate, it may not only clarify the mechanical meanings of deformation of the diaphragm, but also enable us to calibrate the deformation of the diaphragm by measuring the mechanical impact given, or the velocity change of the blast meter. With this in view, an apparatus to cause a sudden change of velocity to the blast meter by mechanical collision was designed and constructed.

6.1. Apparatus for mechanical impact:

As has been certified by the experiment using the high speed camera, time necessary for velocity change of several meters a sec. to the diaphragm was under 0.1ms. Therefore, an apparatus was designed where a falling steel body, which served as a substitute for the diaphragm gauge and to which the diaphragm was fixed on its periphery, might collide with a rigid steel block vertically and rebound. On this occasion, the effective diameter of

the diaphragm has been altered to 50 mm., for the convenience of measuring. The falling body was a thick cylinder with a spherical bottom, and contained the diaphragm fixed in it, as shown in Fig. 18. Four of the six protrusions in symmetrical positions on the outer side of the body served as a guide for the body to fall vertically along the two piano wires of 3 mm. ϕ , extended vertically and tightly by adding tension to them. The other two projections in the opposite positions have been given rhombic cross sections, and are used as a shutter to a light beam, as will be described later. The spherical bottom of the falling body collided with the flat part of the rigid steel block, and the body while rebounding was picked up with the hand, because a second collision would change the deformed shape of the plate. In order to give a large rebounding velocity to the body, the

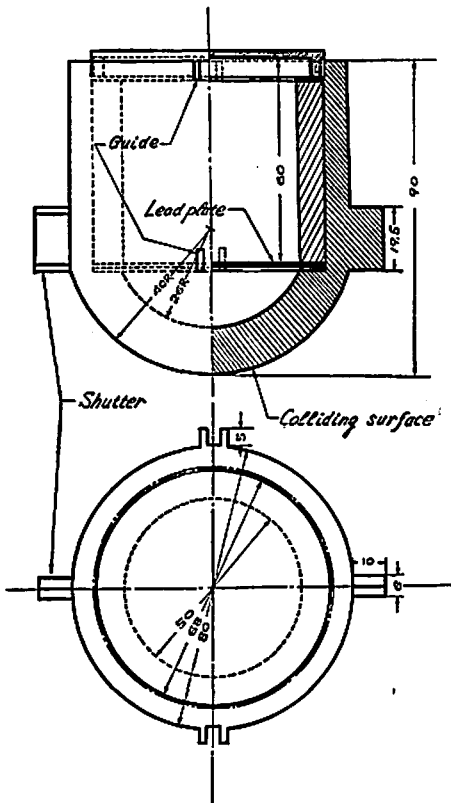


Fig. 18 The falling body

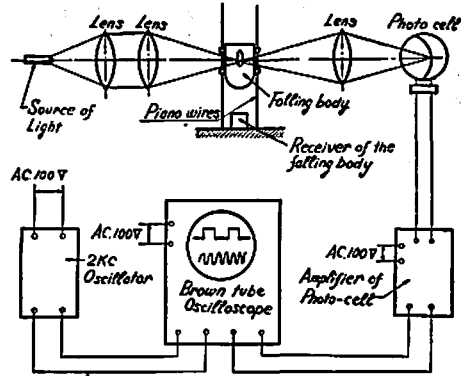


Fig. 19 An arrangement for mechanical impact and an apparatus to measure the velocity change

hard steel block of 63 kg. has been chosen and fastened to the foundation of reinforced concrete with anchor bolts. This arrangement is shown in Fig. 19.

6. 2. Apparatus for measuring the velocity change:

a) The apparatus for measuring the velocity change of a falling body in collision with the steel block is shown in Fig. 19, in which one of the projections of the rhombic cross section was used as a shutter to interrupt the light beam focused on the photo-cell. Only during the interruption of the beam by the protrusion, the photo-cell causes voltage change in its circuit, which is amplified and conducted to one of the vertical terminals of the 2 beam cathode ray oscilloscope; the result shows a rise of its sweep line, corresponding to the time interrupting the beam.

The other vertical terminal of the oscilloscope was connected to the 2 kc. oscillator to give the time mark. By comparing the two beams on the oscilloscope, the interrupted duration of the light beam will be calculated. This duration corresponds to the time in which the falling body passes the distance equal to the length of the protrusions. Thus the velocity of the falling body can be calculated. In our actual case, the protrusion

interrupted the beam twice, that is, on the two occasions of fall and rebound. Thus, because one falling test gives two velocities of fall and rebound, the sum of those velocities is the velocity change of the falling body in the mechanical impact.

b) Though the beam of light was made as well as possible to converge to a point where the shutter cut it, it had an area of about 4 mm. diameter, and moreover did not distribute uniformly in that area. For the reason that, before the protrusion ceased to cut the area of beam, some time had elapsed, the figure on the oscilloscope corresponding to the voltage change of the photo-cell was not a rectangle but a trapezoid, as shown in Photo. 16. As the single sweep apparatus was not used for the oscilloscope, the length of the base of the trapezoid was not clear, but that of its top was measured more clearly, which corresponded to a shorter length than that of the protrusion. This compensating length c to that of the protrusion was determined at 1.25 mm. by an experiment. If the nominal length of the shutter is l and the diameter of the area of light beam d , $(l+d-2c)$ should be used as the effective length of the shutter in calculating the velocity of the falling body.

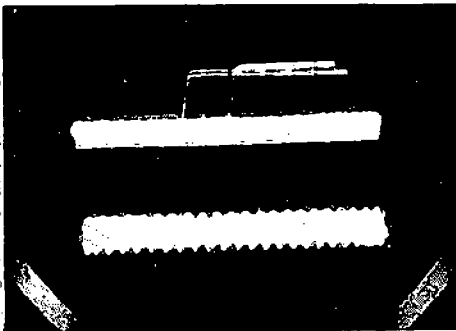


Photo. 16 The voltage change of photo-cell corresponding to the time of fall and rebound of the gauge body

As the shutter cuts the beam twice in the test, two trapezoids appear in the figure of the oscilloscope without regular order of fore or aft; but they can be distinguished from each other, because the length of sweep rise by rebounding must be longer than that by falling.

To calculate the velocity of the body v , we can use the next equation:

$$v = (l + d - 2c) \times f / n,$$

where

- l: length of protrusion = 19.5 mm
- d: diameter of the area of beam = 4 mm
- c: length to be compensated = 1.25 mm
- n: number of waves corresponding to the top length of the trapezoid on the oscilloscope
- f: frequency of the oscillator as a time mark

c) In this falling test, a sliding friction between the piano wires and the guides for sliding exists inevitably, for the body itself falls oscillating, thus causing the friction; and the falling velocity varies so much even if the body was made to fall from the same height. Especially the scattering of the rebounding velocities of the body is very large, because its oblique collision to the stand causes the body to be rotated in rebounding. From these considerations, the data by these tests, in which it was presumed that the rebounding angle was too largely inclined and the ratio of the rebounding velocity to the falling was too small, were omitted in the arrangement.

6.3. Specimens and some miscellaneous items:

The properties of the lead specimen are as follows:

- a) Purity: 98.63 %,
- b) The manufacturing process, as already described.
- c) Tensile strength: 2.2 kg/mm²,
Yield point: 0.8 kg/mm²,

Young's modulus: 1860kg/mm²,

Elongation: 43 %.

Nine thicknesses were adopted in the test with the range of from 0.7 mm. to 4.5 mm. On the surface of the plate, two diameters crossing the center at right angle to each other and five concentric circles with radii of from 5 mm. to 25 mm. at an interval of 5 mm., were drawn to set the measuring points for deformed shape, and for the convenience of fixing the diaphragm on the falling body.

This experiment was carried out not only with circular plates but also with circular plates with concentric holes, which were punched out by a die in order to gain an accuracy for the diameter of the hole and precision for the position.

The measuring method of the thickness of

the plate was as described above in Experiment II.

To decide the deformed shape of the plate, vertical heights and horizontal lengths on the cross points of the two diameters and the five concentric circles were measured exactly by using a reading microscope with three coordinate axes in order to avoid impairing the deformed shape of the plate, though practically they may be measured pretty correctly by slide calipers.

The range of from 1 m. to 4.5 m. at intervals of 0.5 m. was chosen as the falling height of the body, which, however, had no special significance. It only means that the falling velocity was varied to cover some finite range, because it had to be measured in each test.

6. 4. Résumé of the experiments and the:

Table 3 Résumé of the measured data

Film No	Item	Notation	Unit						
				1	2	4	7	11	12
Falling. high			M	2.0	"	"	2.5	"	"
Plate thickness			mm	1.61	1.56	1.58	0.68	0.71	0.80
○ With a hole △ Without a hole				△	△	○	△	○	○
Effective area			mm ²	1978	"	1900			
No. of waves at fall	n_1			7.4	7.0	7.1	6.4	6.1	6.0
No. of waves at Rebound	n_2			12.0	12.0	11.0	9.0	8.7	10.6
Falling velocity	v_1		m/s	4.59	4.86	4.79	5.31	5.57	5.67
Rebounding velocity	v_2		m/s	2.83	2.83	3.09	3.78	3.91	3.21
Velocity change	Δv		m/s	7.42	7.69	7.88	9.09	9.48	8.88
Effective volume			(mm) ³	3185	3086	3002	1345	1349	1520
Effective weight	W		gr	36.12	35.00	34.04	15.25	15.30	17.23
Effective mass	W/g		gr·s ² /cm	3.62	3.57	3.48	1.56	1.56	1.76
Impulse	s		gr·s	27.38	27.45	27.44	14.18	14.79	15.63
Coefficient of rebound	v_2/v_1			0.167	0.582	0.645	0.712	0.702	0.566
Height of the cone	h		mm	4.45	4.72	5.08	5.97	6.59	6.98
Inclination of the cone	$\tan \alpha$			0.227	0.241	0.268	0.307	0.340	0.367

measured date:

The experiments have, from the beginning, been classified into fifteen groups, from *A* to *O*, and here the results of the groups from *K* to *O* are mainly shown because these are more reliable date.

The results measured in the photographs of the oscilloscope out-puts, the calculated data of the velocity change Δv , the impact S given to the plate, and the measured data of the deformed height h of the plate and of the inclination $\tan \alpha$ of the generated cone for test group *L*, are resumed in Table 3 as examples.

6.5. Measurement of duration of collision:²⁶⁾

In some of these experiments of measuring the velocity change, the impact load of collision was also measured, using the combination of wire resistance gauge and a Brown

tube oscilloscope. It aimed at measuring the duration of collision by the mechanical impact test, to compare it with that of shock wave pressure at explosion. The wire gauge was adhered to the protrusion of the steel block receiving the impact, lest the stress wave generated by collision should be disturbed by the reflecting wave on the steel block. In the circuit for measuring strain a single sweep apparatus was used, and was triggered by the voltage change in the circuit of the photocell the moment the falling body sheltered the light beam. Therefore, in these experiments from *A* group to *F* group, the impact load and the velocity change were simultaneously measured by each test of mechanical collision. The general arrangement of the measuring apparatus is shown in Fig. 20, and as an example, a photpgraph of the impact

and the calculated data for the group *L*

No. of Specimen											
14	15	16	20	23	25	26	28	30	33	35	36
"	"	"	"	"	3.0	"	"	"	"	"	"
0.91	0.92	0.89	1.21	1.22	0.70	0.70	0.80	0.81	0.88	0.90	0.89
△	△	○	△	○	△	△	○	○	△	○	○
1978 For mark △						1900 For mark ○					
6.0	5.6	5.1	6.0	5.6	5.8	5.7	5.6	5.9	5.6	5.4	5.8
8.1	9.8	9.5	9.7	9.4	8.4	7.8	9.6	9.1	9.0	9.4	9.9
5.67	6.07	6.67	5.67	6.07	5.86	5.96	6.07	5.76	6.07	6.30	5.86
4.21	3.47	3.58	3.51	3.62	4.05	4.36	3.54	3.74	3.78	3.62	3.43
9.88	9.54	10.25	9.18	9.69	9.91	10.32	9.61	9.50	9.85	9.92	9.29
1800	1820	1691	2394	2318	1385	1385	1520	1539	1741	1710	1691
20.41	20.63	19.17	27.14	26.28	15.70	15.70	17.23	17.45	19.74	19.39	19.17
2.08	2.11	1.96	2.77	2.68	1.60	1.60	1.76	1.78	2.02	1.98	1.96
20.55	20.12	20.01	25.43	25.97	15.86	16.50	16.91	16.91	19.90	19.64	18.21
0.743	0.573	0.537	0.619	0.596	0.619	0.732	0.583	0.649	0.623	0.575	0.585
5.71	5.95	6.39	5.73	6.10	6.55	6.33	7.18	6.98	5.50	5.96	6.12
0.294	0.306	0.336	0.299	0.323	0.343	0.325	0.382	0.367	0.279	0.317	0.318

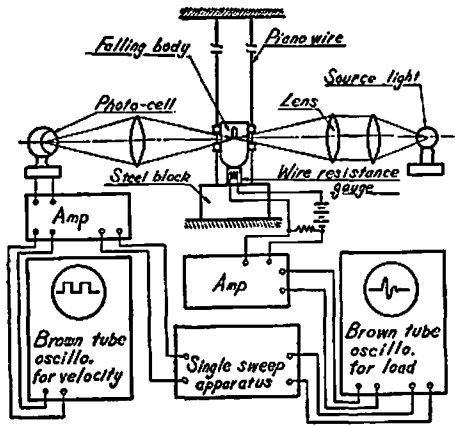


Fig. 20 The general arrangement of measuring apparatus of the impact load and the velocity change

load measured by the oscilloscope is shown in Photo. 17, which denotes the impact very near to a half sine wave. An example of the data of measurement and calculation is resumed in Table 4 with the data of the measurement of velocity change. Both the maximum load and the impulse calculated on this table coincide well with each other. The duration of contact is about 50μ sec. in all collisions and the maximum load is within the range of 10ton~55ton, both of which coincide well with the values calculated by the author on Hertz's contact theory¹⁵⁾. The duration of collision by the mechanical impact test obtained from this measurement is a little shorter than that of shock wave pressure by explosion acting on

Table 4 Résumé of the measured data

Item	Notation	Unit				
	F		1.5-1	1.5-3	1.5-4	2.5-2
No. of waves	n_1		6.2	7.0	6.4	4.8
Time	T_1	ms	3.10	3.50	3.20	2.40
Falling velocity	v_1	M/S	4.12	3.65	3.99	5.32
No. of waves	n_2		10.8	12.0	13.7	8.8
Time	T_2	ms	5.40	6.00	6.75	4.40
Rebounding velocity	v_2	M/S	2.37	2.12	1.89	2.90
Coefficient of rebound	e		0.575	0.579	0.473	0.545
Velocity change	Δv	M/S	6.490	5.770	5.880	8.220
Impulse	$\frac{W}{g} \cdot \Delta v$	kg·s	1.483	1.319	1.344	1.879
Impulse	$\frac{W}{g} \cdot v_1$	kg·s	0.941	0.834	0.912	1.216
Max. load by velocity change	$\frac{W}{g} \cdot v_1 \cdot \frac{\pi}{2}$	ton	29.1	25.7	29.1	38.5
Max. load by strain measured	P_{max}	ton	20.1	21.6	20.9	34.6
Impulse by strain measured	$J_P = \frac{2P_{max}}{\pi}$	kg·s	0.669	0.669	0.659	1.090
Duration of contact	Δt	μ S	52.3	50.8	49.4	49.4
Height of cone	h	mm	4.3	3.6	3.3	4.8
Inclination of cone	$\tan \alpha$		0.212	0.198	0.130	0.226

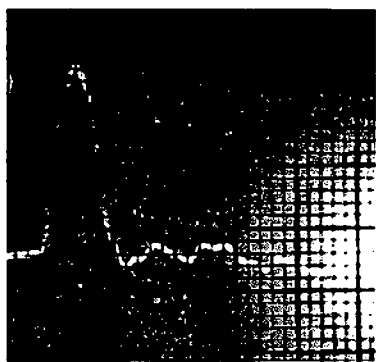


Photo. 17 Load curve at impact test

the diaphragm, and it shows that the results attained by mechanical impact tests are applicable to the calibration of the deformation of the plate under blast type loading. But the

absolute values of the impact loads gained by these measurements are not so sufficiently reliable as the duration, because the wire resistance gauge has the tendency of being affected by magneto-strictive effect at such high strain rates as one shown in these test.³⁰⁾

6.6. Relation between impulse and deformation:

The figures of the diaphragms deformed by mechanical impact with this apparatus have always been found to be similar to cones or frustums of cones, as expected, and are shown in Photo. 18. Therefore, the height of the cone h or the inclination of the conical surface $\tan \alpha$ has been chosen as one of the quantities representing the deformation of

and the calculated data for the group F.

No. of Specimen								
2.5-3	2.5-4	3-1	3-2	3-3	3-4	4-1	4.5-3	4.5-4
5.1	5.0	4.3	4.6	4.6	4.8	4.0	4.7	4.4
2.55	2.50	2.15	2.30	2.30	2.40	2.00	2.31	2.20
5.01	5.10	5.94	5.56	5.55	5.32	6.39	5.54	5.80
9.0	10.4	8.4	9.2	10.4	10.7	9.5	8.4	6.2
4.50	5.20	4.20	4.60	5.20	5.35	4.75	4.20	3.10
2.83	2.46	3.04	2.77	2.46	2.38	2.69	3.04	4.12
0.565	0.482	0.512	0.498	0.444	0.449	0.422	0.500	0.709
7.840	7.560	8.980	8.330	8.010	7.700	9.080	8.480	9.920
1.792	1.728	2.052	1.904	1.831	1.760	2.075	1.961	2.267
1.145	1.165	1.357	1.271	1.268	1.216	1.460	1.266	1.325
34.4	37.6	45.7	40.3	39.8	35.5	50.8	40.2	44.7
43.6	34.1	46.7	41.7	39.2	36.5	40.9	51.6	48.6
1.452	1.040	1.381	1.351	1.233	1.250	1.174	1.623	1.440
52.3	48.0	46.5	49.4	49.4	53.8	41.5	41.4	46.5
4.9	4.9	5.25	5.4	5.4	5.6	6.3	6.5	6.1
0.240	0.206	0.243	0.243	0.244	0.253	0.293	0.290	0.283

the plate. In fact the top of the cone is not sharp pointed but rounded, and the radius of the rounded top is larger on the thick plate

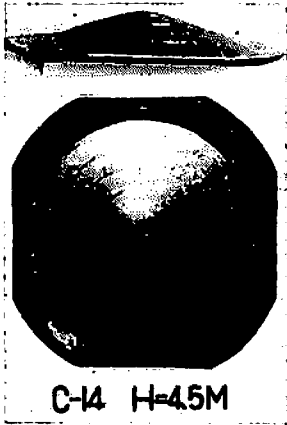


Photo. 18 The deformed shape of the lead circular plate by mechanical impact

than on the thin plate. To be free from errors in measuring the height of the cone owing to such a rounded top, the height of the concentric circle of initial 10 mm ϕ , denoted by h , was measured instead of the total height of the cone h_t . Thus, the height h was rightly related to the inclination of the conical surface $\tan \alpha$. This geometrical relation is shown in Fig. 21.

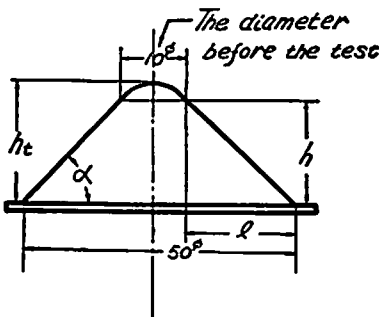


Fig. 21 Relation among h , h_t and $\tan \alpha$

If the velocity change Δv of the blastmeter was gained by the mechanical impact, impulse S received on the diaphragm is $m\Delta v$, where m is mass of the effective area of the plate. Since the effective area of the plate is

constant, m is proportional to the thickness of the plate. To express the impulse without relation to the thickness of the plate, as in measuring the deformation height, we represent the mechanical quantity by the velocity change Δv , which is the sum of the falling velocity v_1 and the rebounding velocity v_2 .

In order to ascertain that such simplification is reasonable, the relations of Δv to h or $\tan \alpha$ have been plotted in Fig. 22 and Fig. 23, for all the test data obtained for the plates of the thickness of 0.7 mm, 1.6 mm, 2.8 mm and 4.5 mm. It is clear that they have generally a linear relation and the noticeable dispersion of this relation in spite of the differences of the plate thicknesses can not be perceived. If it is necessary to observe the effect of the plate thickness in this relation, it can be pointed out that h or $\tan \alpha$ increases with the decrease of the thickness, probably for the reason that, exactly speaking, the bending resistance is not zero and increases with the increase of the plate thickness. In Fig. 22 and Fig. 23, data of only four sorts of the plate thickness among the nine sorts of tested thickness are indicated to avoid an undistinguishableness, liable to be caused by plotting too many points the data gave, but it must be added that the other data also indicate the same tendency.

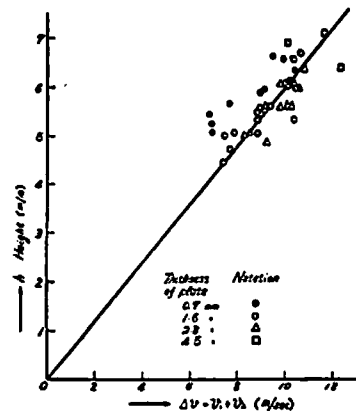


Fig. 22 Relation between the velocity change and the deformed height

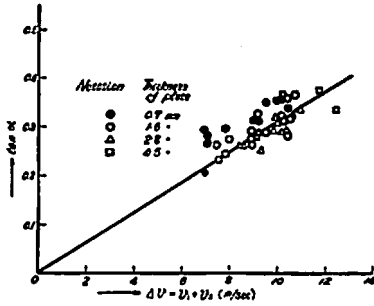


Fig. 23 Relation between the velocity change and the inclination of the cone

Thus, it has been proved to be true that Δv may be used instead of S , in order to manifest an impulse given to the diaphragm without relation to the plate thickness.

6.7. The effect of a central hole:

In order to know how a hole at the center of the plate affects the quantity of deformation h or $\tan \alpha$, data of the deformations of the diaphragms with or without a hole have been plotted together in Fig. 24 and Fig. 25 using the different marks for them. From these two graphs it is noticed that the deformation of the plate with a hole is a little larger than that of the plate without a hole. This fact denotes that, during the deformation, resistance to the radial displacement of the plate is larger in the plate without a hole than in the plate with a hole, but the difference of resistance between them is not so large.

Comparing the two dispersions of deformation Fig. 24 and Fig. 25, it is recognized that the dispersion in data of h or $\tan \alpha$ is smaller for the plate with a hole than for the plate without a hole. The total formed height h_t , though it is not plotted in the figures, dispersed much more than the dispersions in Fig. 24 and Fig. 25, because h_t is affected by the plate thickness as has been described above. Therefore, in order to increase the accuracy of the experiment, in the case of h , it is recommendable to measure

the deformed height using the plate with a hole, in the air, although it can not be used for underwater explosions.

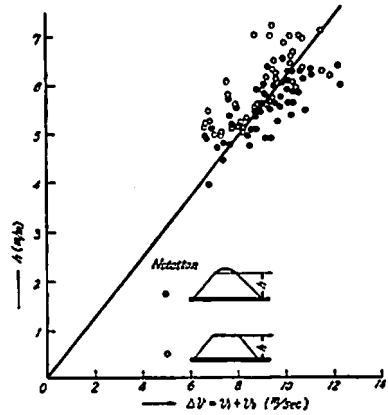


Fig. 24 Relation between Δv and h , using the different marks for the plate with or without a hole

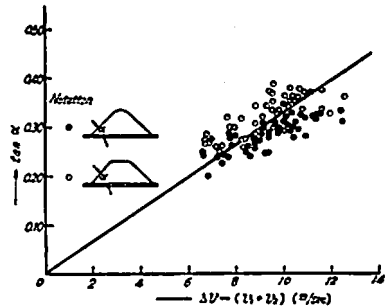


Fig. 25 Relation between Δv and $\tan \alpha$, using the different marks for the plate with or without a hole

6.8. Calculation of calibration curves:

All values of h and $\tan \alpha$ have been plotted to Δv on the graphs of Fig. 26 and Fig. 27, which show that generally a linear relation exist between them. From those data, excluding those dispersed too far apart, as are shown in the graphs, the equation expressing the relation of Δv to h or $\tan \alpha$ has been calculated by the method of least squares, and also the standard deviation for it has been obtained as follows.

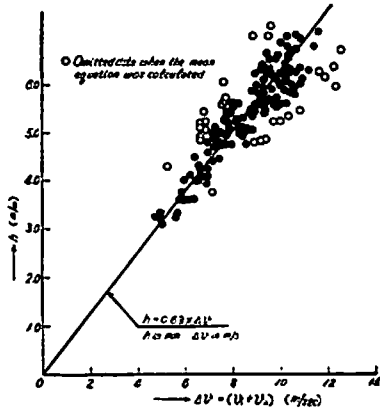


Fig. 26 Velocity change and height of the deformed cone

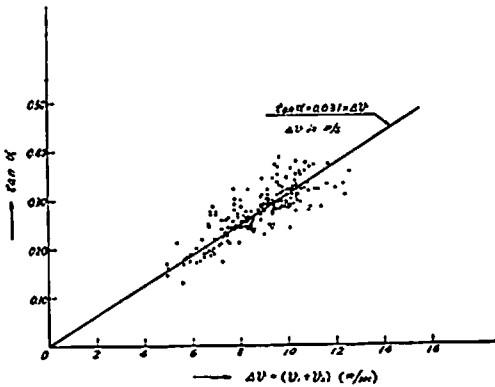


Fig. 27 Velocity change and gradient of the deformed cone

Put $h = k_1 \cdot \Delta v$

where h in mm. and Δv in m/s. are shown. The constant coefficient k_1 is calculated by solving the simultaneous equations,

$$k_1 \sum_{i=1}^n \Delta v_i = \sum_{i=1}^n h_i$$

$$k_1 \sum_{i=1}^n (\Delta v_i)^2 = \sum_{i=1}^n (\Delta v_i \times h_i),$$

where n is the number of the groups of data adopted. From these equations the following two values of k_1 are obtained.

$$k_{11} = 0.6313, \text{ and } k_{12} = 0.6235.$$

Existence of two values of k_1 shows that h and Δv are not in a homogeneous relation, but in the relation of $h = k_1 \cdot \Delta v + b$.

By applying a similar method to the relation of $\tan \alpha = k_2 \cdot \Delta v$, the following two values of k_2 have been calculated.

$$k_{21} = 0.0312, \text{ and } k_{22} = 0.0313.$$

Therefore, empirical equations for h and Δv have been obtained as follows:

$$h = 0.6313 \times \Delta v,$$

and

$$h = 0.6235 \times \Delta v.$$

Similarly the experimental equations for $\tan \alpha$ and Δv are

$$\tan \alpha = 0.0312 \times \Delta v,$$

and

$$\tan \alpha = 0.0313 \times \Delta v.$$

If $\tan \alpha$ is multiplied by the mean value of l , which is the horizontal span of the initial 10 mm. ϕ circle after deformation as shown in Fig. 21, its value must be nearly equal to the value of h in the equation. To check it, using $l = 19.3$ mm., we obtain

$$h' = 19.3 \times 0.0312 \times \Delta v = 0.604 \times \Delta v.$$

The difference between the equations of h and h' is within 5%.

The standard deviation σ of k_1 has been calculated and we have obtained $\sigma = 0.04223$, which shows that the deviation is not so extremely large.

6.9. Sand-heap form of deformation:

The diaphragms of various shapes on the blastmeter are found to deform into various sand-heap forms by the shock wave pressure of explosion in the air. So again, with the apparatus for mechanical impact lead plates of various shapes such as rectangle, square, regular triangle and oval in addition to circle were tested and deformed into various sand-

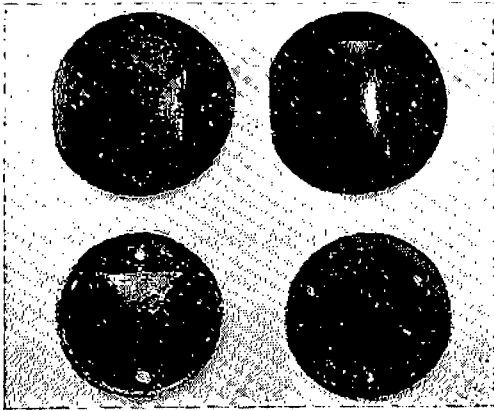


Photo. 19 The depressions of sand heap form of the lead plates by mechanical impact

heap forms similar to those obtained by the explosive tests. These specimens are shown in Photo. 19.

6.10. Deformation by diverging plastic wave:

In all experiments made above, the diaphragms of the gauge are to receive impulse on the outer fixed boundary, and the plastic waves generated there proceed to the center—they are the converging waves. Even in the rectangular bar, the plastic waves are born at the both ends, proceed in one dimension and converge toward the middle point. What will happen when the diaphragm receives impulse at its center and a diverging plastic wave proceeds outwards? To try this, the falling body as shown in Fig. 28 has been constructed. The lead circular plate of 2mm. thickness and 49 mm. diameter was fastened, in the central area of 16 mm. diameter, to the falling body by a 6 mm. ϕ bolt. This was tested with the apparatus for mechanical impact, and the impact gave the diaphragm a deformation into a frustum of a cone, the upper flat part of which was of course fastened to the falling body. The result is shown in Photo. 20. In this case plastic wave generated on the central fixed circle of the body is supposed to proceed outwards, so

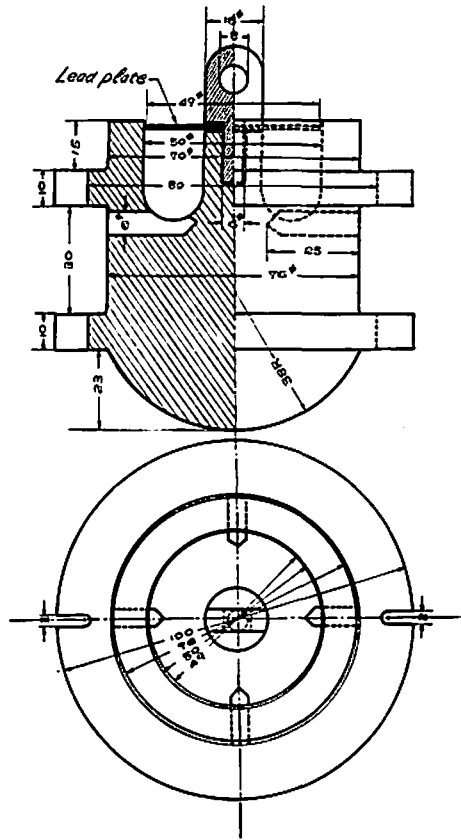


Fig. 28 The falling body to cause a diverging plastic wave to the plate



Photo. 20 The diaphragm deformed into a frustum of a cone by diverging plastic wave

that it is a diverging wave. Therefore, it may well be said that a peculiar sand-heap form of the plastic deformation of the plate is generated by impact not only in the case of converging. but also in the case of diverging plastic wave, of course in the case of the plane wave too which is intermediate. It is to be noticed that the outer periphery of

the plate is waved by a large deformation of the plate, because this kind of deformation is not so stable as in the converging wave, and at last buckling may occur at the periphery of the plate forced by too large deformation.

7. Experiment V, by high-speed flash photographing²⁷⁾

Experiment IV shown that mechanical impact also generates the same deformation of sand heap form on the diaphragm of the blastmeter as does shock wave pressure of explosion. To ascertain if the similar process of deformation of the diaphragm will be generated in both cases, the deforming figures of the plate have been photographed in the process of deformation by high-speed flashes as follows.

7. 1. Apparatus of mechanical impact and the specimens:

In this experiment, the apparatus for mechanical impact and the same specimens as in Experiment IV have been used except for the falling body, which had an enclosed spherical bottom, and the bottom did not permit the diaphragm fixed in the body to be photographed. Therefore a new falling body, which is shown in Fig. 29, has been reconstructed by cutting off both sides of the spherical bottom, through the opening of which the deforming figure of the plate was photographed.

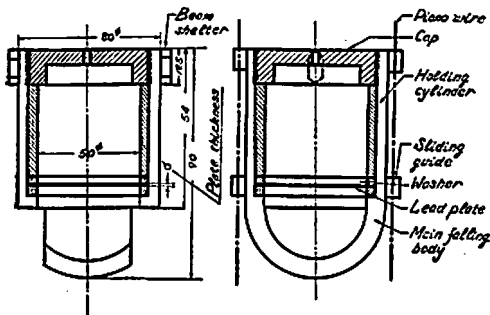


Fig. 29 The falling body for high speed flash photographing

7. 2. Apparatus for high-speed flashing:

The high-speed flash lamp we used, was filled with argon gas, and was made by Mitsubishi Electric Machine Co. at the Itami Research Laboratory. This lamp and the reflecting mirror made by ourselves are shown in Photo. 21. To the terminals at both ends of the lamp was connected the condenser of $6\mu\text{F}$, which was charged and raised to 4500 volts before flashing. This energy was discharged into the lamp and generated an instantaneous flash, induced by the sudden charge aroused in the coil wound the lamp, to which another condenser was discharged by the output of the trigger circuit. By this discharge an illumination of 10^8 lumen is generated for about $5\mu\text{sec}$. The block diagram of the whole apparatus is shown in Fig. 30. The voltage changes in the circuit of photocell, when the light beam is cut by the protrusion of the falling body, served as the trigger for flash. The same arrangement for photo-cell and light system was used as in Experiment IV. As only a frame of photograph a test is taken by every flash, timing of flash must be finely adjusted by shifting in each test in order to photograph different stages of the deforming figure. For this purpose a fine adjusting apparatus for trigger time was set in front of the trigger circuit.

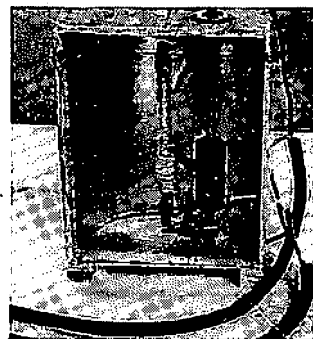


Photo. 21 High speed flash lamp in the reflecting mirror

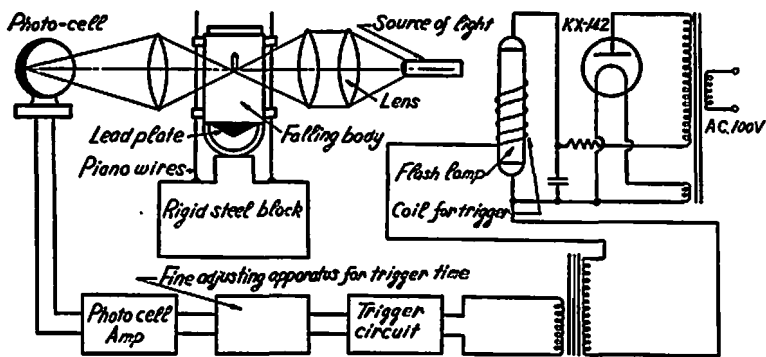


Fig. 30 Arrangement of high speed flash photographing in mechanical impact test

7. 3. Photographs taken:

By the apparatus described above were taken many sheets of photograph, eight of which have been arranged in regular order in regard to the height of deformation of the plate, as is shown in Photo. 22. But the time-lags between them could not be known, because they were photographed separately in those eight tests. By observing the deforming figures of the plate in these photographs, it is confirmed that the plastic wave generated by mechanical impact on the fixed boundary proceeds to the center of the plate, leaving the central part flat, as did the deformation by explosive pressure. Therefore, it is affirmed that a linear relation between the height of the deformed plate and velocity change of the falling body by the mechanical impact test is usable as a calibration curve for the height of the deformed plate by the explosion test.

8. Experiment VI: Comparison of the deformation of plates with and without a hole.²⁹⁾

In Experiment IV of mechanical impact test, a linear relation has been decided between the deformation of the circular lead plate with or without a center hole and the momentum change given to it. Because the total height of cone is affected by the thickness of the plate, but not the vertical dis-



Photo, 22 Deforming process of the lead circular diaphragm by mechanical impulse

placement of the circle of 10 mm. or the inclination of the cone, it may seem to be better for raising accuracy to measure the latter. This measurement, however, is tedious, besides it is not free from inaccuracy. Therefore, as a result of Experiment IV, it is recommended to use the lead circular plate with a center hole as the diaphragm, in order to measure more accurately and easily the depression of the plate. The experiment described here has been carried out in order to see if it is truly so in explosion test too.

8. 1. Experimental method:

The deformations of the lead circular plates with and without a hole were compared by the pass-through method. A new blast-meter, the effective area of which is 50 mm. in diameter, has been constructed so that the results therefrom can be compared with those obtained from the mechanical impact test.

The thickness of the plate was measured at the four symmetrical points on the central circle of 30 mm. diameter, and each of them was maintained within its nominal thickness ± 0.03 mm. All the rest about the specimens was the same as Experiment II.

The diaphragms have been prepared for seven groups of thickness, which are 0.7mm., 0.9mm., 1.2mm., 1.6mm., 2.0mm., 2.4mm. and 2.8 mm. The explosive distance was changed eight times, at intervals of 5 cm.

from 15 cm. to 50 cm. Only some appropriate combinations of thickness and distance were tested to avoid the rupture of the plate or too small deformations.

8. 2. Experimental results:

The number of the diaphragms tested is 161. Of all specimens that have been tested, the measured data of h , $\tan \alpha$ and h_t of only 18 have been tabulated in Table 5 as an example. From all these data, $\tan \alpha$ has been plotted against the explosive distance in Fig. 31, which does not prove any regular relation

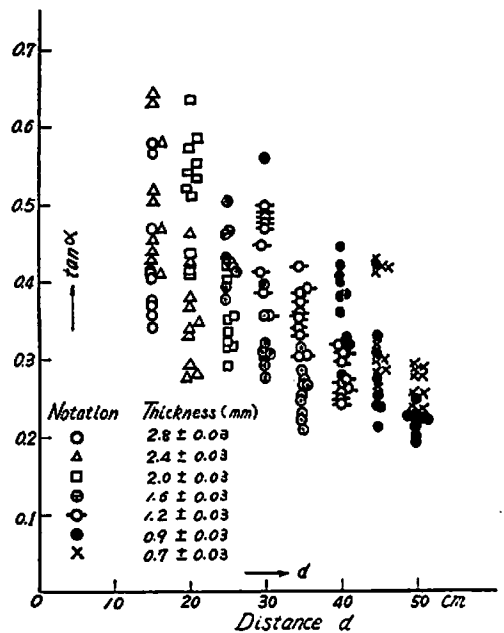


Fig. 31 Relation between the explosive distance and the inclination of the cone

Table 5 Measured data of deformation of

Item	Notation	Unit						
Test piece No.			2-1	2-2	2-3	2-4	2-5	2-6
○ With hole △ Without hole			○	○	○	○	○	○
Height	h	mm	8.61	9.15	8.05	10.14	8.50	6.54
Inclination	$\tan \alpha$		0.469	0.505	0.434	0.578	0.641	0.343
Explosive distance	d	cm	15	"	"	"	"	20
Thickness	δ	mm	2.408	2.418	2.408	2.413	2.422	2.408
Height of the top	h_t	mm						

to exist between them.

The impulse S given to the plate by explosive pressure, is given by the velocity change Δv incurred to the plate, multiplied by the mass m of the effective area of the plate; hence,

$$S = m \cdot \Delta v = \rho A \delta \cdot \Delta v$$

where ρ is the density of lead, A and δ the effective area and the thickness of the plate respectively.

From the results of Experiment IV, equations of $h = k_1 \times \Delta v$ and $\tan \alpha = k_2 \times \Delta v$ have been given, and then the following relations hold:

$$\delta h = \frac{k_1}{\rho A} S \quad (2)$$

$$\text{or } \delta \tan \alpha = \frac{k_2}{\rho A} S \quad (3)$$

where k_1, k_2, ρ and A are given constants. Therefore δh and $\delta \tan \alpha$ are quantities proportional to S .

The logarithm values of the mean $\delta \tan \alpha$ for the same explosive distance have been plotted to each explosive distance in Fig. 32, which shown the existence of a fine linear relation between them, whether the plate has a center hole or not.

The similar relation between δh of the plate with a hole and the explosive distance is

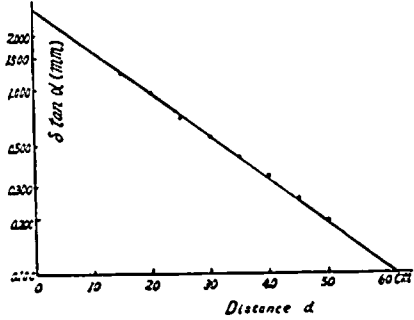


Fig. 32 Relation between $\delta \tan \alpha$ and explosive distance

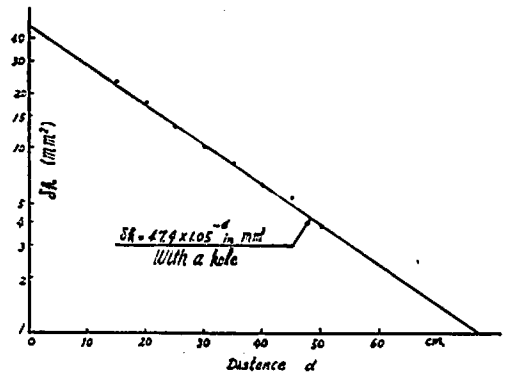


Fig. 33 Relation between δh of the plate with a hole and the explosive distance

shown in Fig. 34. This linear relation, using the method of least squares, can be expressed by

$$\delta h = 47.4 \times 1.05^{-d} \text{ mm.}^2 \quad (4)$$

where d is in cm. Its standard deviation is

the diaphragms by the pass through method

No. of Specimen											
2-7	2-10	2-12	2-13	2-15	2-16	2-17	2-18	2-19	2-20	2-21	2-22
○	○	○	○	△	△	△	△	△	△	△	△
7.12	8.08	6.86	8.34	9.62	11.86	8.58	8.14	12.13	6.87	6.83	5.76
0.378	0.435	0.363	0.452	0.508	0.641	0.444	0.415	0.637	0.345	0.346	0.292
"	"	"	"	15	"	"	"	"	20	"	"
2.409	2.396	2.421	2.415	2.402	2.410	2.397	2.423	2.417	2.411	2.417	2.418
				10.43	12.79	9.38	8.77	13.13	7.29	7.31	6.48

0.407.

Similar diagrams to δh and δh_t of the plates without a hole are shown in Fig. 34 and Fig. 37 and we have the empirical equations for them as follows;

$$\delta h = 44.8 \times 1.05^{-d} \text{ mm.}^2, \quad (5)$$

$$\text{and } \delta h_t = 48.3 \times 1.05^{-d} \text{ mm.}^2. \quad (6)$$

Their standard deviations are 0.631 and 0.640. By examining these standard deviations in the three cases, it was proved quantitatively that, adopted for the diaphragm with a center hole, the blastmeter by the pass-through method gives a superior accuracy.

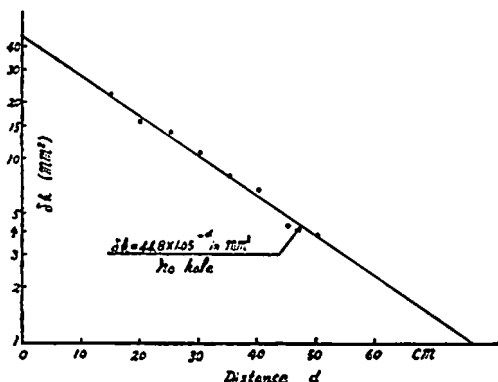


Fig. 34 Relation between δh of the plate without a hole and the explosive distance

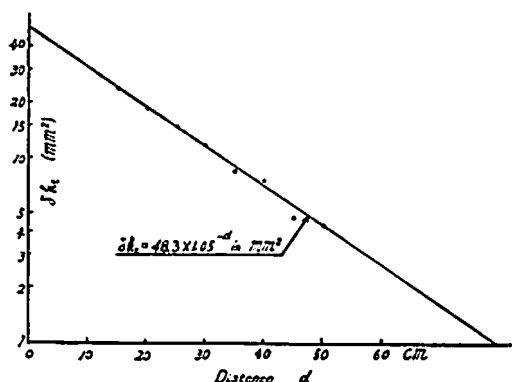


Fig. 35 Relation between δh_t and the explosive distance

III. CONCLUSION

From the above experiments and analyses following conclusions have been deduced.

(1) The phenomenon that the circular lead diaphragm of the blastmeter deforms

into a conical shape under strong shock wave pressure by explosives of high detonating speed in the open air, is not to be attributed to a special property of lead, but is common to all ductile metals, and is attributed to the special process of plastic deformation. Under such loading the diaphragm deforms always into a sand-heap form, which depends on the form of the fixed boundary.

(2) In the blastmeter, which is widely used in Japan as well as abroad, the lead diaphragm deforms into a cone within a short time of about one millisecond owing to a shock wave pressure of about $100 \mu\text{s}$. duration by explosion of 50 gram TNT, for the explosive distances ranging from 10cm. to 50 cm., which are the distances that the shock wave pressure is well expected to distributed uniformly on the plate. If pressure on the plate continues for a much longer time than is just necessary for the total deformation of the plate, it deforms into a semi-sphere and any intermediate duration gives an intermediate shape of deformation.

(3) The mechanical process of deformation of the metal diaphragm into a sandheap form is as follows:

The diaphragm gains uniform velocity relative to the boundary of the blastmeter by shock wave pressure or mechanical impulse in an instant. The parallel motion of the diaphragm so produced is next constrained at its periphery by the fixed boundary, where at first a plastic deformation of the plate is generated and proceeds to the center of the plate, leaving the central undeformed part flat for sometime. And such a phenomenon is caused not only by the converging plastic wave alone, but also by the diverging one, of course, also by certain one-dimensional plastic waves. However, the deformation by the converging wave is stable whilst that by the diverging one is unstable.

(4) Therefore, the height of the deformed diaphragm, the shape of which is either conical or semi-spherical, is not a simple function of the maximum pressure to which the plate has been exposed. The height or the inclination of the conically deformed diaphragm is proportional to the total impulse given to the plate.

(5) Moreover, the top of the cone of the deformed diaphragm is not sharp-pointed but has the partly rounded top, the radius of which differs according to the thickness of the plate used. To avoid errors induced by the rounded top, it is advisable to measure the inclination of the cone or the height of the frustum of cone, which is gained by a circular lead plate with a center hole and from which the impulse given to the blastmeter is to be calculated. These values, as the calibration by the mechanical impact test has given, are:

$$h=0.63 \times \Delta v \quad (h \text{ in mm, } \Delta v \text{ in m/sec.),}$$

$$\tan \alpha = 0.031 \times \Delta v \quad (\Delta v \text{ in m/sec.})$$

where h is the height of the frustum of cone, $\tan \alpha$ the inclination of the cone and Δv the velocity change given to the plate. The impulse is obtained by the product of Δv calculated by these equations and the mass of the effective area of the plate.

(6) It has followed from the above experiments that the diaphragm of the blastmeter may be treated as a membrane, and not as a rigid plastic plate, under blast type loading. Hudson's analysis is appropriate as far as his assumptions and his final results, are concerned. On the other hand, the author's analysis fully explains the process of the deformation well.

The conclusion described above, also, gives a fundamental concept concerning "Explosive Forming", which is recently being given much attentions to, as a possible substitute for mechanical press of large metal plates and

about behaviors of the damages of steel structures under blast type loading. There is also another application. In a severe collision of rigid bodies, the diaphragm gauge can be used to measure the impulse between them. Using round bars fixed at both ends as gauges, we have the advantage of being able to decide simultaneously the direction of collision, too.

ACKNOWLEDGEMENT

I thank the publication committee of Journal of the Industrial Explosives Society, Japan, for its kindness that it permits the republication of this paper, which is a reduced copy of Vol. IX, No. 2 of Memoirs of the Faculty of Engineering, Kumamoto University and does not contain the part of mathematical analysis.

The foregoing experiments were carried out with the financial helps of the Asahi Chemical Industry Co., the Japan Carlit Co., and the Teikoku Kakohin Manuf. Co. In concluding the paper, the author wishes to express his sincere gratitude to Prof. Yamamoto, Prof. Kondo and Prof. Uemura, University of Tokyo, Prof. Sudo, Chuo University, Dr. Fukuyama, the Asahi Chemical Industry Co. and Prof. Yanagimoto, Kumamoto University, who gave him valuable advices and kind encouragements throughout the course of the investigation, and also to express his hearty thanks to the assistants, Mr. Ogata and Mr. Mikuni for having helped him in carrying out the experiments.

REFERENCES

- (1) R. H. Cole: Underwater Explosion, p. 157 & p. 408 (1948)
- (2) A. H. Bebb: Undex. 131 (1945)
- (3) Jahres-berichte, D. C. T. R. Bd. III, S. 88
- (4) W. Gliwitzki: ZVDI Bd. 80, S. 687, (1936)
- (5) H. Busch: Brennstoff-chemie, Nr. 23/24, Bd. 36, S. 372 (1956)

- (6) W. Hoffmann und G. Meier: Z. Metallkunde, Bd. 45, Nr. 8, S. 508 (1954)
- (7) H. Busch: Explosivstoffe, Nr. 314, S. 50 (1959)
- (8) Shinji Yamaga: J. Soc. Ordnance and Explosives, Japan, Vol. 31, No. 6
- (9) Hatsutaro Suzuki: Kaigun, Kaken-ko, No. 331
- (10) Ikuo Fukuyama: Lecture at the Industrial Explosives Soc. Japan, Oct., 1950
- (11) H. J. Cough and G. A. Hankins: J. Roy. Aeronaut. Soc., Vol. 39 (1935)
H. G. Hopkins and W. Prager: J. Mech. Phys. Solids, Vol. 2, p. 1 (1953)
H. G. Hopkins and A. J. Wang: J. Mech. Phys. Solids, Vol. 3, p. 117 (1955)
- (12) Toyotaro Suhara: Rept. of Aeronaut. Research Inst., Vol. 5, No. 6
- (13) G. E. Hudson: J. Appl. Physics, Vol. 22, No. 1, p. 1 (1951)
- (14) D. S. Clark and G. Datwyler: Proc. of A. S. T. M., Vol. 38, Part II, p. 98 (1938)
M. J. Manjoine: J. of Appl. Mechanics, Vol. 11, p. 211 (1944)
- (15) H. Hertz: J. Math., Vol. 92 (1881)
- (16) B. Hopkinson: Phil. Trans. Roy. Soc. A 213, p. 437 (1914)
- (17) Kiyota and Sudo: Lecture at the Industrial Explosives Soc. Japan, April, 1955
- (18) H. G. Hopkins and W. Prager: Z. angew. Math. Phys., Bd. 5, S. 317 (1954)
- A. J. Wang and H. G. Hopkins: J. Mech. Phys. Solids, Vol. 3, p. 22 (1954)
- (19) E. W. Parkes: Proc. Roy. Soc. (London) A 228, p. 462 (1955)
- (20) R. Hill: The Mathematical Theory of Plasticity
Prager and Hodge: Theory of Perfectly Plastic Solids
- (21) H. Kolsky: Stress Waves in Solids, p. 166 (1953)
- (22) Kenkichi Kiyota: Tech. Reports of Kumamoto Univ., Vol. 1, No. 1 (1951)
- (23) Kenkichi Kiyota: Tech. Reports of Kumamoto Univ., Vol. 1, No. 2 (1952)
- (24) H. Sudo and K. Kiyota: J. of Industrial Explosives Soc. Japan, Vol. 12, No. 34 (1952)
- (25) Kenkichi Kiyota: Lecture at Japan Soc. of Mech. Engineers, April, 1952
- (26) Kenkichi Kiyota: Pre-Print of Japan Soc. of Mech. Engineers, April, 1955
- (27) Kenkichi Kiyota: Pre-Print of Japan Soc. of Mech. Engineers, Oct., 1955
- (28) Kenkichi Kiyota: Lecture at the Industrial Explosives Soc. Japan, April 1956
- (29) K. Kiyota and I. Fukuyama: Lecture at the Industrial Expl. Soc. Japan, Nov., 1956
K. Kiyota and I. Fukuyama: Lecture at the Industrial Expl. Soc. Japan, April, 1958
- 30) K. Kiyota: Pre-print of Japan Soc. of Mech Engineers, Oct., 1957